PROCEEDINGS OF SPIE

SPIEDigitalLibrary.org/conference-proceedings-of-spie

Photoacoustic microscopy of neovascularization in three-dimensional porous scaffolds in vivo

Xin Cai, Yu Zhang, Li Li, Sung-Wook Choi, Matthew R. MacEwan, et al.

Xin Cai, Yu Zhang, Li Li, Sung-Wook Choi, Matthew R. MacEwan, Junjie Yao, Chulhong Kim, Younan Xia, Lihong V. Wang, "Photoacoustic microscopy of neovascularization in three-dimensional porous scaffolds in vivo," Proc. SPIE 8581, Photons Plus Ultrasound: Imaging and Sensing 2013, 858128 (4 March 2013); doi: 10.1117/12.2005236

SPIE.

Event: SPIE BiOS, 2013, San Francisco, California, United States

Photoacoustic Microscopy of Neovascularization in Three-Dimensional Porous Scaffolds *In Vivo*

Xin Cai,[1] Yu Zhang,[2] Li Li,[3] Sung-Wook Choi,[4] Matthew R. MacEwan,[1] Junjie Yao,[1]

Chulhong Kim,[5] Younan Xia,[2] and Lihong V. Wang[1,*]

[1]Optical Imaging Laboratory, Department of Biomedical Engineering, Washington University in St. Louis, St. Louis, Missouri 63130

[2]Wallace H. Coulter Department of Biomedical Engineering, Georgia Institute of Technology and Emory University, Atlanta, GA 30332, USA

[3]Wellman Center for Photomedicine, Massachusetts General Hospital and Harvard Medical School, 55 Fruit Street, Boston, MA 02114, USA

[4]Department of Biotechnology, The Catholic University of Korea, Bucheon 420-743, Korea

[5]Department of Biomedical Engineering, University at Buffalo, The State University of New York, Buffalo, NY 14260, USA

ABSTRACT

It is a challenge to non-invasively visualize *in vivo* the neovascularization in a three-dimensional (3D) scaffold with high spatial resolution and deep penetration depth. Here we used photoacoustic microscopy (PAM) to chronically monitor neovascularization in an inverse opal scaffold implanted in a mouse model for up to six weeks. The neovasculature was observed to develop gradually in the same mouse. These blood vessels not only grew on top of the implanted scaffold but also penetrated into the scaffold. The PAM system offered a lateral resolution of ~45 μm and a penetration depth of ~3 mm into the scaffold/tissue construct. By using the 3D PAM data, we further quantified the vessel area as a function of time.

Keywords: Three-dimensional scaffold; photoacoustic microscopy; tissue engineering; neovascularization; biomedical imaging.

1. INTRODUCTION

Tissue engineering aims to improve or replace biological functions, leading to applications for wound healing. Angiogenesis is one of the most important steps in the process of wound healing. Three-dimensional (3D) scaffolds can provide physical supports and adjustable microenvironments for tissue regeneration[1] Thus, non-invasive *in vivo* imaging of the vascularization process in scaffolds is critical for optimizing the properties of scaffolds, including biocompatibility, biodegradability, mechanical strength, porosity, pore size, and interconnectivity.[2] However, a significant difficulty in scaffold imaging is the lack of an imaging modality with high resolution, deep penetration, and strong contrast. For example, laser-scanning optical microscopy (LSM), including confocal and multi-photon microscopy, has high resolution. However, due to strong light scattering, especially in the presence of blood, LSM is typically limited to

* Corresponding author: lhwang@biomed.wustl.edu

Photons Plus Ultrasound: Imaging and Sensing 2013, edited by Alexander A. Oraevsky, Lihong V. Wang,
Proc. of SPIE Vol. 8581, 858128 · © 2013 SPIE · CCC code: 1605-7422/13/$18 · doi: 10.1117/12.2005236

several hundred micrometers penetration in tissue. Micro-computed tomography (micro-CT) can penetrate up to several centimeters. However, it is ionizing irradiation and provides poor contrast for soft tissue, which limits its *in vivo* applications. So, new non-invasive imaging modalities with high resolution, deep penetration, and strong contrast are needed for 3D scaffold-based samples.

Photoacoustic microscopy (PAM) is attractive for imaging scaffolds non-invasively. Recently, some investigations for PAM imaging and monitoring of 3D scaffold-based samples have been reported.[3-6] PAM detects photoacoustic waves generated from absorbed laser irradiation.[7] The non-ionizing irradiation in PAM imaging is safer than ionizing X-rays in micro-CT. Additionally, hemoglobin, the primary carrier of oxygen in blood, exhibits a strong intrinsic optical absorption contrast in the range of visible light.[8-9] This unique feature allows label-free PAM to map the vasculature and to avoid possible alterations to the hemodynamics caused by exogenous angiographic agents.[10]

Here, we report the capability of PAM to monitor neovascularization in an inverse opal scaffold implanted in a mouse model for up to six weeks. The neovasculature was observed to develop gradually in the same mouse. By using the 3D PAM data, we further quantified the vessel area as a function of time.

2. MATERIALS AND METHODS

2.1 Preparation of inverse opal scaffolds

Poly(D, L-lactide-co-glycolide) (PLGA) inverse opal scaffolds (lactide/glycolide=75/25, Mw≈66,000-107,000, Sigma-Aldrich) were fabricated by following our published procedures.[11] Briefly, gelatin (Type A; Sigma-Aldrich) microspheres with uniform sizes were produced using a simple microfluidic device. Then, gelatin lattices were obtained after thermal fusion of cubic-close-packed gelatin microspheres. Finally, PLGA inverse opal scaffolds were fabricated by templating against the gelatin lattices.

2.2 Animals and implantation of scaffolds

All animal experiments were performed in accordance with protocols approved by the Washington University Department of Comparative Medicine and the Animal Studies Committee. Athymic nude mice at the age of 4-5 weeks were obtained from Harlan and housed in the animal facility at Washington University. The scaffolds (4 mm diameter × 1.5 mm height) were sterilized in 70% ethanol for at least 2 h prior to implantation, and then were implanted subcutaneously in the ears of the mice. For implantation, firstly, a parasagittal incision was made in the ear root of each animal approximately 0.5 cm to the head. Secondly, a subcutaneous pocket was created lateral to the incision by using blunt dissection. Then, a scaffold was inserted into the pocket. Finally, the skin incision was closed with 9-0 Ethilon suture (Ethicon, Somerville) and secured using VetBond dermal adhesive (3M, St. Paul). During the surgeries and PAM experiments, the animals were anesthetized by administration of gaseous isoflurane (2%, Butler Inc., Dublin) and aseptically prepared.

2.3 Histology

At 2, 4 and 6 weeks post-implantation, the scaffolds were explanted, fixed in 3.7% formaldehyde (Sigma-Aldrich), dehydrated in a graded ethanol series (70–100%), embedded in paraffin, and sectioned in thickness of 5 μm. Then, the samples were stained with hematoxylin/eosin and observed under Nanozoomer (Hamamatsu).

2.4 Photoacoustic microscopy

The schematic of the system has been reported in previous work.[3, 8] For photoacoustic excitation, a dye laser (CBR-D, Sirah) pumped by a Nd:YLF laser (INNOSLAB, Edgewave) was employed to provide 7-ns laser pulses with a repetition rate up to 5 kHz. For photoacoustic detection, a focused ultrasonic transducer with 50 MHz central frequency (V214-BB-RM, Olympus NDT) was employed. The optical and ultrasonic foci were configured coaxially and confocally. This system could achieve 45 μm lateral resolution, 15 μm axial resolution, and more than 3 mm penetration depth. It took ~5 min to acquire a 3D image with dimensions of 6 × 6 × 3.75 mm^3, which covered the whole scaffold sample.

3. RESULTS

Fig. 1a shows the SEM image of typical PLGA inverse opal scaffolds. It is clear that the inverse opal scaffold had a uniform and well-arranged pore structure. This structure can provide good interconnections between adjacent pores, facilitating cell/tissue activities throughout the entire scaffold. Fig. 1b is a typical photograph, showing a PLGA inverse opal scaffold with a pore size of ~200 μm in diameter was implanted subcutaneously in the ear of nude mouse (one scaffold per ear per mouse).

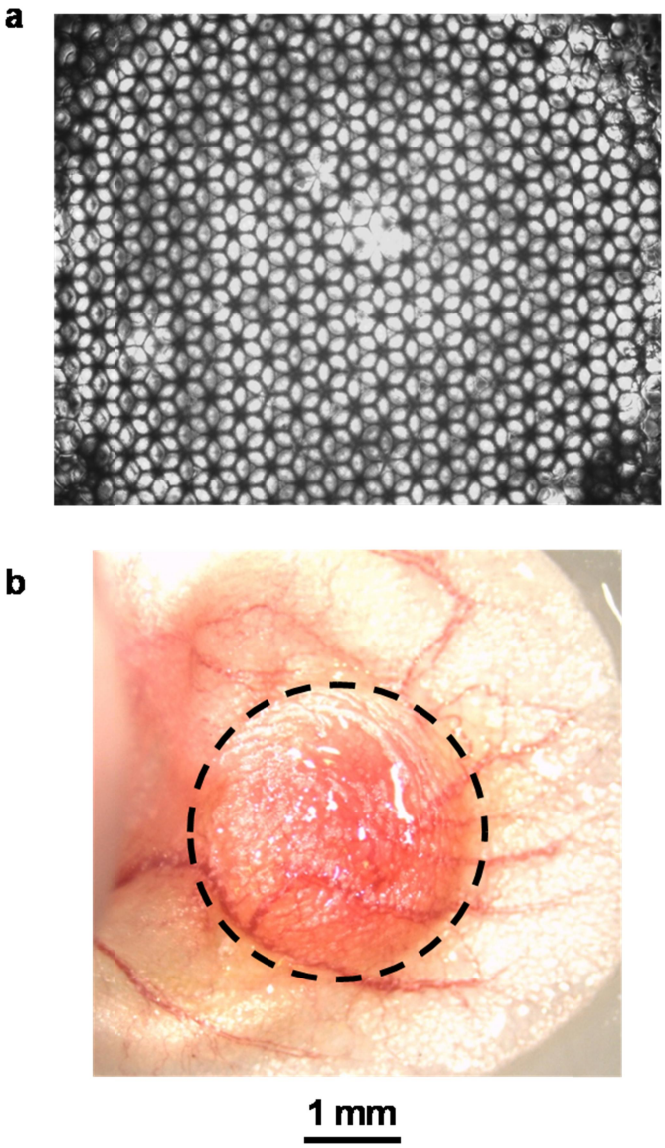

Fig. 1. (a) A typical SEM image showing a PLGA inverse opal scaffold. (b) A typical photograph showing the scaffold (marked by a dotted circle) implanted subcutaneously in the ear of a nude mouse.

Three mice with scaffold implantation were monitored by PAM at an excitation wavelength of 570 nm up to 6 weeks post-implantation. In this study, the PLGA polymer itself could not generate sufficient photoacoustic signals, and thus only vasculature was imaged by PAM due to the strong optical absorption of hemoglobin. As shown by the sagittal

maximum amplitude projection (MAP) images (side view) from one of the mice in Fig. 2, a–d, the imaging depth covered the thickness of the scaffold (1.5 mm), and the density of blood vessels increased during these 6 weeks. At 1 week post-implantation, the area of the scaffold (indicated by the white dotted trapezoid) could be clearly resolved due to the absence of blood (Fig 2a.). These blood vessels not only grew on top of the implanted scaffold but also penetrated into the central region of scaffold.

Another three mice with scaffold implantation were sacrificed and subjected to histology analyses at the same time points as the PAM imaging. Fig. 3, a–c, shows typical hematoxylin and eosin (H&E) stained sections from the central region (200–800 μm below the surface) of the scaffolds at 2, 4 and 6 weeks post-implantation, respectively. A few blood vessels (indicated by arrowheads) with small diameters could be observed starting at Week 2 (Fig. 3a), and they grew both in number and area during 6 weeks (Fig. 3, b–c). These observations were consistent with the PAM images

To further demonstrate the capability of PAM, the area of blood vessel as a function of time was quantified from three-dimensional (3D) PAM data. The area of blood vessels at each time point was normalized against that at Week 2. The quantification results (Fig. 3d) show that the normalized vessel area at Week 6 was ~7 times larger than that at Week 2. Similar results could be obtained from the histological data.

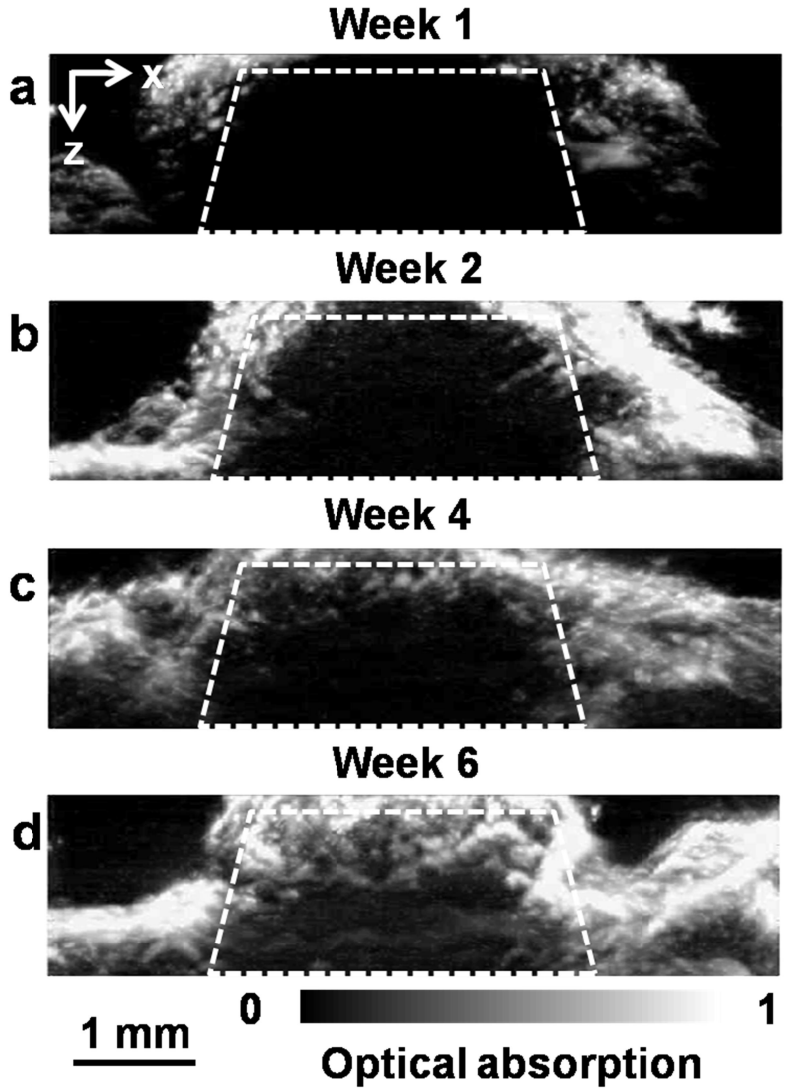

Fig. 2. Chronic PAM images showing the development of neovasculature in an inverse opal scaffold *in vivo*. (a–d) Sagittal MAP images at 1, 2, 4, and 6 weeks post-implantation, respectively. The dotted trapezoid indicates the area where the scaffold resided.

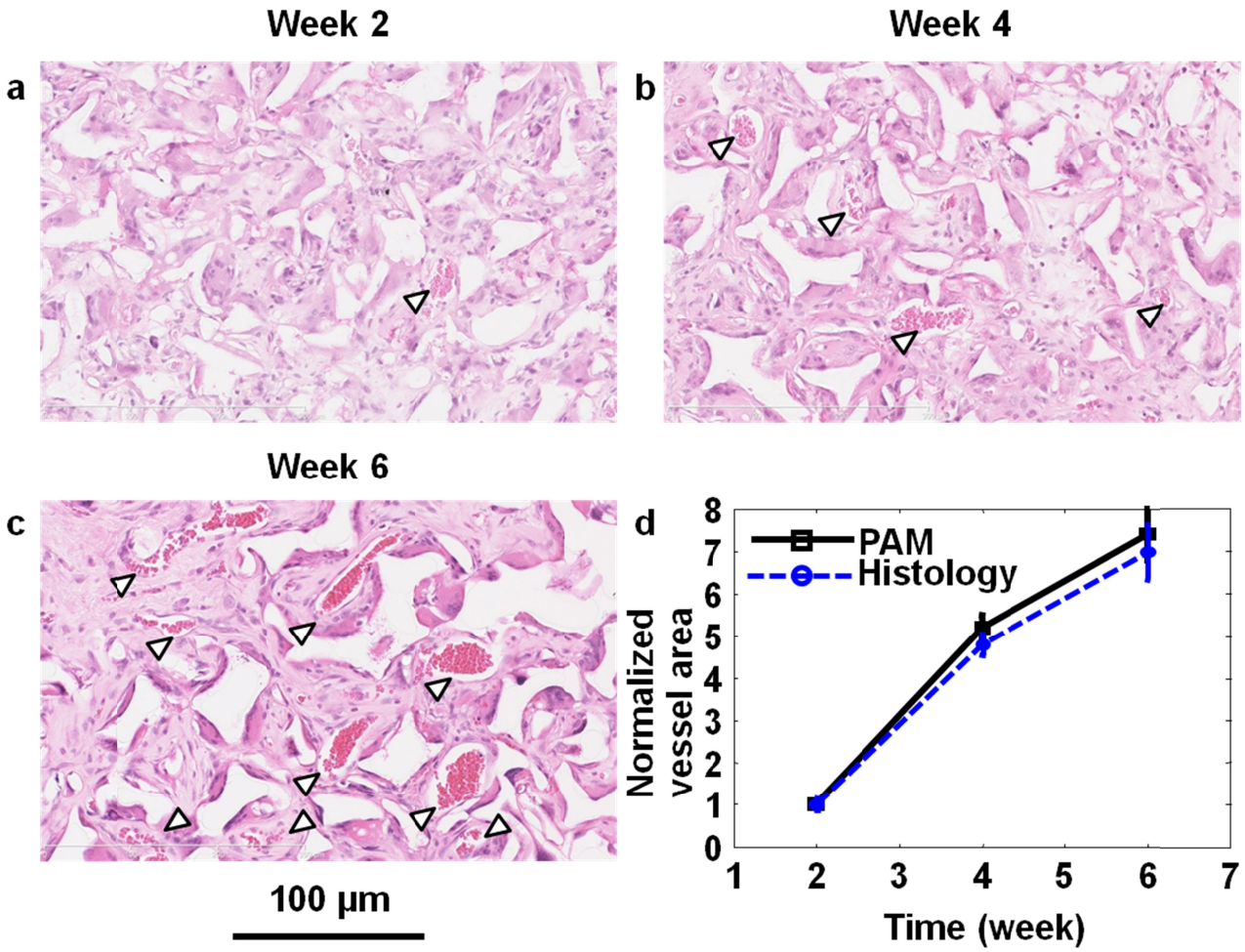

Fig. 3. Histological images showing the development of neovasculature in an inverse opal scaffold. (a–c) Hematoxylin and eosin stained sections of the central region (200–800 µm below the surface) of the explanted scaffold post-implantation at 2 weeks (a), 4 weeks (b), and 6 weeks (c), respectively. Arrowheads indicate blood vessels. (d) Comparison of histological analyses and PAM quantification. The results were presented as mean ± standard error (n=3).

4. CONCLUSION

We have demonstrated that neovascularization in scaffolds can be monitored non-invasively *in vivo* by PAM for more than 6 weeks. PAM quantifications agree well with traditional invasive, labor-intensive histological analyses. Our results suggest that PAM is a promising tool for *in vivo* monitoring of scaffold-induced angiogenesis.

5. ACKNOWLEDGMENTS

Our work was also sponsored by NIH grants R01 EB000712, R01 EB008085, R01 CA140220, R01 CA157277, R01 CA159959, U54 CA136398, and DP1 EB016986—NIH Director's Pioneer Award. L.V.W. has a financial interest in Microphotoacoustics, Inc. and Endra, Inc., which, however, did not support this work. Others claim no competing financial interests.

REFERENCES

[1] R. Langer, J. P. Vacanti, "Tissue engineering," *Science* 260, 920–926 (1993).

[2] M. Lovett, K. Lee, A. Edwards, D. L. Kaplan, "Vascularization strategies for tissue engineering," *Tissue Eng Part B: Reviews* 15(3), 353–370 (2009).

[3] Y. Zhang, X. Cai, S.-W. Choi, C. Kim, L. V. Wang, Y. Xia, "Chronic label-free volumetric photoacoustic microscopy of melanoma cells in three-dimensional porous Scaffolds," *Biomaterials* 31, 8651–8658 (2010).

[4] Y. Zhang, X. Cai, Y. Wang, C. Zhang, L. Li, S. W. Choi, L. V. Wang, and Y. Xia, "Noninvasive photoacoustic microscopy of living cells in two and three dimensions through enhancement by a metabolite dye," *Angew Chem Int Ed* 50(32), 7359–7363 (2011).

[5] X. Cai, B. S. Paratala, S. Hu, B. Sitharaman, and L. V. Wang, "Multiscale photoacoustic microscopy of single-walled carbon nanotube-incorporated tissue engineering scaffolds," *Tissue Eng Part C: Methods* 18(4), 310–317 (2012).

[6] X. Cai, Y. Zhang, L. Li, S. W. Choi, M. R. MacEwan, J. Yao, C. Kim, Y. Xia, and L. V. Wang, "Investigation of neovascularization in three-dimensional porous scaffolds *in vivo* by a combination of multiscale photoacoustic microscopy and optical coherence tomography," *Tissue Eng Part C: Methods* 19(3), 196–204 (2013)

[7] C. Kim, C. Favazza, L. V. Wang, "*In vivo* photoacoustic tomography of chemicals: high-resolution functional and molecular optical imaging at new depths," *Chem Rev* 110, 2756–2782 (2010).

[8] H. F. Zhang, K. Maslov, G. Stoica, L. V. Wang, "Functional photoacoustic microscopy for high-resolution and noninvasive *in vivo* imaging," *Nat Biotechnol* 24, 848–851 (2006).

[9] J.-M. Yang, C. Favazza, R. Chen, J. Yao, X. Cai, K. Maslov, Q. Zhou, K. K. Shung, and L. V. Wang, "Simultaneous functional photoacoustic and ultrasonic endoscopy of internal organs *in vivo*," *Nat Med* 18(8), 1297–1302 (2012).

[10] S. Hu, L. V. Wang, "Photoacoustic imaging and characterization of the microvasculature," *J Biomed Opt* 15(1), 011101 (2010).

[11] S.-W. Choi, J. Xie, and Y. Xia, "Chitosan-based inverse opals: three-dimensional scaffolds with uniform pore structures for cell culture," *Adv Mater* 21, 2997–3001 (2009).